Journal of molecular lipids, 259, 154-166

A novel pH-sensitive liposomes to trigger delivery of afatinib to cancer cells: Impact on lung cancer therapy

Alanood S. Almurshedi, Mahasen Radwan, Samiah Omar, Ayodele A. Alaiya, Mohamed M. Badran, Hanaa Elsaghire, Imran Y. Saleem, Gillian A. Hutcheon.

Abstract

A novel drug delivery systems based on cationic (CL) and pH-sensitive liposomes (PSL) for tyrosine kinase inhibitor afatinib (AFT) were developed to enhance tumor-targetability against NSCLC cells and therapeutic effect. Optimal lipid to drug ratio was selected to prepare AFT-loaded PSL and CL with desirable physiochemical properties based on particle size, drug encapsulation efficiency (EE%), stability and release profiles. Moreover, antitumor activity was performed *in vitro* on human lung cancer cells (H-1975) using a WST-1 assay and Annexin-V apoptosis assay. The mean particle size of the liposomes was less than 100 nm, and EE% was more than 50% with lipid to drug ratio of 1:0.5. Stability data showed that PSL and CL were physically stable for 1 months at 4 and 25 ^{o}C. *In vitro* drug release study demonstrated the sustained release of AFT at pH 7.5; while PSL exhibited fast drug release in pH 5.5. This effect revealed that PSL showed pH-sensitive release behaviors. In addition, the *in vitro* cytotoxicity study was employed for AFT-loaded PSL due to optimal characterizations. Thus, *in vitro* anticancer activity revealed that AFT loaded-PSL triggered apoptosis in H-1975 cells. In addition, the inhibitory effect towards H-1975 and HCC-827 was observed, indicating, which indicated high antitumor activity of AFT-loaded PSL. Then, PSL might potentially create practical clinical strategies for better targetability and delivery of AFT for treatment of lung cancer.

Key words: Afatinib, pH-sensitive liposomes, *In vitro* release, Anticancer activity, Lung cancers

1. Introduction

Cancer is a foremost problem of disease worldwide to human health in recent years. Moreover, lung cancer becomes a serious danger to human health, it is about 1.38 million cancer-associated mortality in males and females in recent decades [1-2]. The incidence of lung cancer has increased significantly in recent years in Kingdom of Saudi Arabia and United Kingdom due to the increased prevalence of cigarette smoking [3-4]. Approximately 85% of lung cancer diagnoses are classified as non-small cell lung cancer (NSCLC) and the remaining 15% small cell lung cancer (SCLC) [6]. The unsatisfactory effects after treatment of lung cancer patients using conventional approaches such as surgical resection, radiation, and chemotherapy were perceived [6]. The majority of chemotherapy administration is intravenous, causing pronounced side effects due to their systemic drug distribution. Moreover, the bioavailability of orally administrated anticancer agents is usually compromised by the first-pass metabolism [7]. The cytotoxic effects of chemotherapeutic agents against normal cells, according to dose-response effects, have been recorded, leading to the patient's frail and death [8]. Therefore, the targeted delivery of anticancer drugs has become a focus of scientific research. NSCLC treatment can be improved by targeted delivery of chemotherapeutic agent (s) to suppress the major signaling pathways involved in lung cancer. Then the targeted delivery of anticancer drugs directly into the lungs can increase their accumulation in tumor cells and reduce adverse side effects [9]. To date, numerous epidermal growth factor (EGFR) targeting agents have been approved, including gefitinib, erlotinib, and lapatinib; however, both primary and acquired resistance are significant clinical problems [10]. Afatinib (AFT) is a novel, potent, small-molecule tyrosine kinase inhibitor (TKI), which is now marketed (2013), as a film-coated oral tablet as a dimaleate salt. AFT is an especially effective treatment for nonsmall

cell lung cancer (NSCLC) [11]. AFT has ability to bind covalently and irreversibly to the intracellular TK domain, preventing intracellular signaling [12]. By targeting ErbB family receptors, AFT blocks a wide spectrum of cancer-associated ErbB-driven pathways, and thus has broader antitumor activity against receptors with acquired mutations that are resistant to the first generation of TKIs [13]. AFT exposed at low concentration in the tumor cells, which reduced their clinical uses [14]. Therefore, the targeted delivery of AFT has become a focus of scientific research. Nanomedicine is extensively used due to their intrinsic properties such as improved cancer therapy with reduced toxicity. The nanoparticles may be considered as a promising antitumor delivery system for AFT, which may trigger its delivery to the cancer tissues [15]. The liposomes were the interest type of nanomedicine for clinical application in the field of cancer therapy [16]. In addition, they have ability to target tumor tissues via an enhanced permeation and retention (EPR) effect [15]. Liposomes are suitable carriers for pulmonary drug delivery owing to their capacity for targeting to specific cells/tissues [17]. Although drug-loaded liposomes can extend *in vivo* circulation and increase chemotherapeutic activity, they may also be limited targeting and fast cleared [18]. It has been reported that pH-sensitive liposomes have received great attention due to their efficient accumulation in the tumor cells [19]. It has been described that tumor tissues exhibited an acidic condition (pH 5.0-6.5) than normal tissues (pH 7.4-7.5) [20]. Therefore, pH-sensitive liposomes were able to deliver the drugs into the tumor cells when the pH value is lower than the normal tissue. Therefore, it may be expected that pH-sensitive liposomes are more efficient for the delivery of AFT than conventional liposomes due to their fusogenic character [21]. pH-sensitive liposomes could increase the intracellular delivery of their content in cancer cells [20-21]. To the best of our knowledge,

only one study investigated AFT nanoparticles in term of polymeric micelles as a pulmonary delivery system that improved the therapeutic efficacy in HER2-overexpressed HCT-15-induced tumors [22].

In this study, we have prepared three types of liposomes, pH-sensitive liposomes compared with conventional and cationic liposomes containing AFT to study their cancer targeting. An HPLC method was developed and validated for AFT for *in vitro* analysis. The liposomes were characterized in term of particle size distribution, zeta potential and encapsulation efficiency. The surface morphology of the desired liposome was observed by TEM. Moreover, the drug release of AFT was investigated for pH sensitivity (pH 5.5) and prolonged circulation (pH 7.4). The stability studies of these liposomes were performed at a different temperature. Afterward, the NSCLC cells (H-1975 cells) were selected for the assessment of antitumor activity of the optimum liposomes using a colorimetric WST-1 assay and flow cytometry. Moreover, the apoptosis in different cells like H-1975, HCC-827 and H-1650 was established after incubation with liposomes.

2. Materials and methods

2.1. Materials

AFT (99.8% purity) was purchased from Green Stone Swiss Co., Limited. 1,2-distearoyl-sn-glycero-3-phosphocholine [18:0] (DSPC), 1,2-dioleoyl-sn-glycero-3-phosphoethanolamine [18:1] (DOPE), 1,2-dioleoyl-sn-glycero-3-phosphocholine [18:1] (DOPC), and 1,2-dioleoy-3-trimethylammonium-propane Chloride salt (DOTAP) were kindly gifted by Avanti Polar Lipid. Cholesteryl hemisuccinate (CHEMS) was purchased from Avanti Polar Lipid. H1975, H-1650, and HCC827 cells were obtained from the American Type Culture Collection (ATCC, Manassas, VA, USA). Cells were maintained

111 at 37°C and 5% CO2 in RPMI 1640 medium (GIBCO®, SIGMA-ALDRICH, Saint Louis,
112 USA) containing 10% fetal bovine serum (FBS) and1% antibiotic/antimycotic which were
113 purchased from (GIBCO®, InvitrogenTM, Carlsbad, USA). All other reagents and
114 chemicals were of analytical grade.

115 **2.2. HPLC assay of AFT**

116 2.2.1. HPLC instrumentation

117 A Water Breeze2™ HPLC system (Waters Corporation, Milford, U.S.A) was used
118 for method development. The HPLC system equipped with an automated sampling system
119 (Waters™ 2695 Plus Autosampler, USA) at 4°C and a photodiode array detector
120 (Waters™ 2998, USA). The HPLC system was examined by "Breeze2 (Water™)"
121 software. AFT was analyzed using mobile phase that consisted of A: 0.1% triethanolamine
122 and 1% acetonitrile in HPLC water (pH= 6), and B: acetonitrile and 10% methanol at a
123 flow rate of 1 mL/min. The mobile phase flowed over a reversed-phase C18 column
124 (Water™, 3 x 150 mm, 3.5 µm particle size) coupled with a C18 guard cartridge (4×2.0
125 mm) and maintained at 50 ºC. The injection volume of each AFT sample was 10 µl and
126 detected by the UV detector at 253 nm. All the operations were carried out at room
127 temperature.

128 2.2.2. HPLC assay

129 A stock solution of AFT was prepared in methanol at a concentration of 1 mg/ml
130 and stored in 4.0 ml amber glass vials at -20°C. Serial dilutions in mobile phase were
131 performed in the range of 0.01 to 25 µg/ml to produce a standard calibration curve and
132 stored at -20°C. A daily standard calibration curve (n=3) ranging from 0.01 to 25 µg/ml

was prepared to determine the unknown AFT concentrations for entrapment efficiency and drug release.

2.2.3. Method validation

The validation of HPLC method was conducted according to the International Conference on Harmonization (ICH) guidelines. The following items were considered for validation: linearity, accuracy, precision, specificity, limit of detection (LOD), limit of quantification (LOQ) and robustness. Three standard calibration lines were prepared at different times (3 months) to evaluate the linearity, precision, accuracy, and stability of the method.

Linearity was assessed by calculating a regression line by plotting the peak area of AFT vs. the AFT concentration ranging from 0.01 to 25 µg/ml.

The accuracy was determined via the analysis of multiple replicates (n = 6) of AFT concentration. The accuracy of the method was expressed in term of bias.

The precision of a quantitative method was determined by repeatability as intra-day precision by an analysis of three replicates of AFT concentrations over the same day. Inter-day precision was determined by the analysis of three replicates of various AFT concentrations over three different days. The results were expressed as the relative standard deviation (RSD%).

Low, medium, and high concentration quality control (QC) samples at concentrations of (100, 1,000 and 10,000 ng/ml AFT, respectively) were analyzed, on three distinct occasions within at least 3 months, as before described.

The LOD and LOQ were determined from the calibration curve obtained using six replicates that were closest to the LOQ. The following equations were used:

156 $$LOD = 3.3\ \sigma/S \quad \text{Eq. 1}$$

157 $$LOQ = 10\ \sigma/S \quad \text{Eq. 2}$$

158 LOD and LOQ were determined based upon the slope (S) of the calibration curve
159 and least standard deviation obtained from the response (σ). It has a low limit of
160 quantitation (5 ng/ml) with satisfactory specificity, no matrix interference was observed.
161 These findings demonstrated that the assay has good selectivity.

162 **2.3. Preparation of liposomes**

163 Different types of AFT-loaded liposomes were fabricated by thin-film hydration
164 method followed by extrusion as described previously [23]. Non-targeting liposomes (NL)
165 were prepared using DSPC, DOPC, and DOPE at molar ratios of 3: 3: 10. Moreover, three
166 parts of the 10 parts of DOPC of the total liposomal contents were replaced by DOTAP or
167 CHEMS to form cationic and pH-sensitive liposomes, respectively. The AFT was added
168 to the lipids at ratios of 0.25:1, 0.5:1, 0.75:1, 1:1, 1.25:1 and 1.5:1 (w:w), respectively. The
169 composition of the liposomes was presented in Table 1. Briefly, AFT and lipids were
170 dissolved in chloroform, in a round bottom flask following by evaporation to obtain dried
171 thin film at 55 ^{o}C using a rotary evaporator (Buchi Rotavapor R-200, Switzerland). The
172 resulting lipid film was hydrated with the proper volume of phosphate buffer saline (PBS;
173 pH 7.4) by gently mixing for 30 min at 55 ^{o}C to produce multilamellar vesicles (MLVs).
174 The liposomes were subjected to extrusion through polycarbonate membranes with two
175 pore sizes (200 and 100 mm) using a discontinuous extruder (Liposo-Fast™ Avestin Inc.,
176 Ottawa, Canada). The liposomes were extruded 5 times through a polycarbonate membrane
177 with a pore size of 200 nm following by 21 times through 100 nm at low pressure (200
178 psi). The three types of plain liposomes were prepared similarly. The final formulations
179 were stored for overnight at 4°C.

2.4. Physicochemical characterization of liposomes

2.4.1. Particles size distribution and zeta potential

The mean vesicle sizes, size distribution and the zeta potential (ζ) were characterized by dynamic light scattering (DLS) at 25 ^{o}C with a fixed angle of 137° using a Zetasizer Nano ZS (Malvern Instruments Ltd., UK). The liposomes were appropriately diluted with purified and filtered water (0.2 μm pore size) prior to the measurements. The mean vesicle diameters were the averages of five measurements. All measurements were done in triplicate.

2.4.2. Encapsulation efficiency

Due to the poor solubility of AFT, the free AFT occurred in two forms in the external phase of the liposomal dispersion like free undissolved and free dissolved AFT. The free undissolved AFT was separated from the liposomes using light centrifugation. Meanwhile, the supernatant (encapsulated and free dissolved AFT) were filled into centrifuge tubes and ultra-centrifuged at 40000 rpm at 4 ◦C. The clear supernatant which contained the free dissolved AFT was collected. The total AFT regard to the sum of both encapsulated and free AFT that is existed in the liposomal preparation. The concentration of total AFT was determined after dissolving and disrupting of the liposomal dispersion in methanol and triton x-100 using a vortex mixer, followed by centrifugation for 15 min. The clear supernatant which contained the total AFT was then transferred to a new tube and kept at 4 ◦C until analysis.

The drug encapsulation efficiency (EE%) was calculated using the total drug content of liposomal (AFT_{total}) dispersion and un-entrapped drug content of the dispersion (AFT_{free}). The EE% of all the formulation was calculated by using the following formula:

$$EE\% = \frac{AFT_{total} - AFT_{free}}{AFT_{toal}} x100 \quad \text{Eq. 3}$$

2.4.3. Morphology of liposomes

The morphology of selected liposomes was visualized by transmission electron microscope (TEM) using a JEM-2100 electron microscope (Jeol, Tokyo, Japan). Briefly, a drop of diluted liposomes was applied to a copper grid and the excess liquid was removed using filter paper. The samples were air-dried for 15 min and observed by TEM.

2.4.4. Stability study

The physical stability of the selected liposomes was conducted to monitor the physical stability of AFT loaded liposome formulations (Table 2). All liposomal formulations were stored in glass vials at 4±1 °C and 25°C ± 2°C for a period of one month. The stability was evaluated by measuring the average particle size, ζ and PDI during the storage. The AFT content was evaluated by HPLC. The physicochemical stability of the freshly prepared formulation (at day1) was used as the control and the AFT content on day 1 was normalized to 100%.

2.4.5. *In vitro* drug release

In vitro release profile of AFT from of NL, CL, and PSL (selected liposomes) were evaluated using the Franz diffusion cell system (FDC-6, LOGAN, Instruments Corporation, USA). The experiments were conducted in 7 ml of PBS buffer (pH 7.4 and 5.5) with 0.2% Tween 80 to maintain sink condition. The cellophane dialysis membranes (molecular weight cut off: 12-14 KDa) were soaked before use in distilled water at room temperature for 12 h prior to use to ensure its wetting. An aliquot of 100 µL liposomes was added into donor chambers, ensuring there were no air bubbles under the membrane. The receptor compartment consisted of PBS at pH 7.4 for all liposomes and pH 5.5 for PSL at

37 °C, and stirring at 150 rpm. Samples of 500 μL were withdrawn at various time intervals up to 24 h, and replaced immediately with the equal volume of fresh re-heated PBS. The amount of AFT in each sample was analyzed by HPLC. The experiments were performed in triplicate. The data of *in vitro* AFT release were fitted to various kinetic equations, including zero order, first order, Higuchi's model and Korsmeyer Peppas plot and R^2. Then, n values (diffusion exponent) were calculated for each linear curve obtained by the regression analysis of each kinetic equation [24].

2.5. Antitumor activity studies

2.5.1. Cell proliferation assay, WST-1

The *in vitro* cytotoxicity of AFT compared to different chemotherapeutic agents (carboplatin, gemacitabine and paclitaxel) was determined using WST-1 using NSCLC cells (H-1975 cells). In brief, the cells were seeded into 96-well plates at a density of 10^4 cells/well and incubated overnight in culture medium. Afterward, different concentrations of 1, 5, 10, 20, 40 and 80 μM were added to each well and incubated for additional 24 h. At the end of the treatment, a 10 μl of cell proliferation reagent WST-1 kit was added and incubated for 4 h at 37 ^{o}C. The intensities of photometric metabolite (formazan) were measured at 450 nm using an xMark™ Microplate Absorbance Spectrophotometer (Bio-Rad Laboratories, Inc., Hercules, CA, USA). The results are expressed as the IC50, which was obtained graphically using SigmaPlot 10 (SYSTAT Software, Inc., San Diego CA, USA).

2.5.2. Annexin-V apoptosis assay

Cell death was assessed using the Vybrant® Apoptosis Assay kit and flow cytometry. The H-1975 cells were seeded in six-well plates at 7 x 10^4 per well and

incubated overnight. Then, the cells were treated with pure AFT (control) and AFT loaded PSL at concentrations of 0.5, 1, 3, 5 and 8 μm for 24 h after dilution with culture medium. After treatment, the cells were harvested by trypsinization and centrifuged, and re-suspended in PBS. The cells were stained with Alexa Fluor® 488 Annexin V/propidium iodide (PI) and analyzed using the flow cytometer. The percentage of cell death was determined using FACS-Calibur™ apparatus and CellQuest Pro software (Becton-Dikinson Biosciences, Franklin Lakes. NJ, USA). Moreover, the apoptosis in different cells like H-1975, HCC-827 and H-1650 was tested after application of NL, CL and PSL at 0.25, 0.5, 0.75, 1 and 2 μM. Furthermore, the percentage of cell death in the wells containing the free drug and PSL following a 48 and 72h incubation period was subsequently compared with the results of 24 h incubation at 0.25, 0.5, 0.75, 1 and 2 μM.

2.6. Statistical analysis

Quantitative data were expressed as the mean ± SD of at least three replicates. The Student's *t*-test and one-way analysis of variance (ANOVA) using IBMSPSS Statistics 21 was used to assess multiple comparisons between different methods and times. The level of confidence was set as 95%.

3. Results

3.1. HPLC assay

Three HPLC methods have been described for AFT quantification in dosage forms [25]. This method has been reported by Vejendle *et al*, which demonstrated a lack of sensitivity with LOD (60 ng/ml) and a longer run time (20 min). Therefore, A new sensitive HPLC method for AFT analysis was developed in the current study. This method was used

to quantify the AFT concentration for its *in vitro* studies. The method was determined to be specific for AFT in the matrix with no interfering peaks.

It was identified in our laboratory that the maximum absorbance for AFT is at 206 and 253 nm. While, the HPLC analytical methods reported in the literature detected AFT at 252, 258 or 268 nm. Therefore, the detection wavelength of 253 nm was used for a better sense of AFT in the HPLC in this study. As shown in Fig. 1, the average retention time was 2.4 min, with no interfering peaks in chromatogram A (the blank) and chromatograms B, C (AFT). The obtained results indicated the specificity of the HPLC assay method. It should be mentioned that, during the *in vitro* studies, there was no interfering peaks from the NP ingredients co-eluted with the AFT peak, which further confirmed the specificity of the method.

3.2. Method validation

A calibration curve of the peak area of AFT vs. the various AFT concentrations, in the range of 0.01 to 25 µg/ml was conducted. The regression equation of the line was obtained ($y = 360232x + 56.95$) resulting in the correlation coefficient (R^2) of 0.9999. The results indicated the quality of the curve (data not shown). Therefore, there was a good linear relationship between the AFT peak area and its tested concentrations.

The analytical method was validated in terms of linearity, precision, and accuracy. Linearity was assessed using a calibration curve to investigate the ability of this method to get a proportional response to the different concentrations. Based on the concentrations used ranged from 10 to 250000 ng/m, in triplicate, the linearity was evaluated and a calibration curve was constructed.

294 The LOD was determined to be 10 ng/ml and the LOQ was 5 ng/ml, with the
295 corresponding CV values of 1.8 and 0.93 %, respectively (Table 2).
296 For precision and accuracy of sample analysis, AFT standard solutions of three
297 replicates were prepared in triplicate, and analyzed on the same day (repeatability) or in
298 three different days (intermediate precision). Tables 3 showed that the precision did not
299 exceed the required RSD value with maximum RSD value was < 1.98 %. Analysis of
300 variance of the data indicated no significant difference (p =0.401) in the slopes, intra- and
301 inter-day of the calibration curves. The results confirmed the reproducibility of the assay.
302 The accuracy was more than 99.9 %.
303 The method was found to be robust, since small variations in the method conditions
304 had a negligible effect on the chromatographic behavior of the AFT. The results indicated
305 that changing of the HPLC system or the C_{18} column had no effect on the chromatographic
306 behavior of AFT. Even a small change in the mobile phase composition did not
307 significantly change the peak area of the drug used for this method.
308 3.3. Particle size distribution and zeta potential
309 This study aims to evaluate the incorporation of AFT to CL and PSL compared to
310 NL (control liposomes) for the design of an efficient anticancer delivery system. The
311 obtained liposomes were characterized in terms of the mean particle size, PDI and ζ values
312 using DLS and electrophoretic light scattering (Data not shown). The particle size of the
313 liposomes were ranged from 46 to 57 nm and values of PDI were less than 0.2, which
314 indicate narrower size distribution indicating no aggregation. Regarding ζ, the liposomes
315 presented high values according to the increasing lipid to the drug ratios, until the ratio was
316 1:0.5 (Fig. 2). The AFT-containing liposomes exhibited more positive ζ than liposomes

without AFT, which proposes that the addition of DOTAP increased the amounts of AFT in the liposomes. In case of NL, the positive ζ was low and after the incorporation of the drug, ζ increased by approximately two-fold until 1:0.5 of lipid to the drug ratio. CL possessed great values of positive ζ ranging from 38.9 mV for the blank to 48.4 mV for the ratio of 1:0.5. However, PSL exhibited negative values of ζ, due to CHEMS and decreased with the increasing the drug to lipid ratios (Fig. 2).

3.4. Encapsulation efficiency

The effect of the lipid to drug ratio on the encapsulation of AFT is indicated in Fig. 3. As the lipid to AFT ratios increased, the amount of the drug was increased to a certain extent and then decreased. The highest values of the encapsulated AFT were on lipid to drug ratio, 1:0.5, the EE values were 43, 50, and 52 % for NL, PSL, and CL respectively. As expected, the amount of AFT in the liposomes would increase with increasing of drug concentration. After reaching the maximum capacity of AFT, EE values were decreased with more AFT. However, the amount of free drug increased ($P< 0.05$) significantly, thereby notably decreasing the EE%.

According to the obtained results, a lipid to drug ratio 1:0.5 in all tested liposomes was selected for further studies due to the high value of EE%. On the contrary, PSL at a lipid to drug ratio of 1:1 showed the lowest EE%.

3.5. Morphology of liposomes

TEM images of PSL are presented in Fig 4. The images showed that PSL were a spherical shape. In addition, the existence of multilamellar structure was well visualized inside PSL (Fig. 4). It has been reported that the protonated CHEMS showed a lower hydration ability than CHEMS at neutral pH, while the protonated amino group of

phosphatidylethanolamine (PE) exhibited greater hydration ability, thus enhancing the immiscibility between PE and CHEMS and causing formation of a heterogeneous system [23].

3.6. Stability study

The short-term stability of the selected liposomes of lipid:drug ratio of 1:0.5 was investigated for up to 30 days at 4 ± 1 ^{o}C and 25 ± 2 ^{o}C. This ratio was chosen due to the highest EE% of AFT. There was no significant change in the particle size, PDI, ζ and AFT EE% of liposomes during the stability study at 4°C compared to the initial preparation ($p > 0.05$). However, at 25 ^{o}C, the particle size of the liposomes after storage for 30 days as 47.5±2.3 to 75±3.3 nm, 53.8±2.6 to 84±15.9 nm and 55.3±1.2 to 79.5±2.5 for CL, PSL and NL respectively. However, liposomes were still smaller than 100 nm. There was no appreciable change in PDI over 30 days. The ζ at 4°C and 25^{o}C for 30 days exhibited insignificantly different (p =0.141) compared to the initial formulation. The EE% of AFT after storage at 4°C and 25°C for 30 days was slightly decreased but was still higher than 90% and 80%, respectively, of the initial formulations (Fig.5).

3.7. *In vitro* release study

To evaluate the *in vitro* drug release behaviors of AFT from CL and PSL compared to NL, these nanoliposomes were incubated in pH 7.4 PBS solutions at 37 ^{o}C in (Fig. 6). Moreover, to determine the pH sensitivity of PSL, the drug release behavior under pH 5.5 was also investigated, and pH 5.5 was selected to mimic the tumor pH (Fig. 6). As weakly acidic environments are presented in the endosomal and lysosomal of tumor cells [26].

The AFT release rate was relatively slow in neutral pH 7.4, just reaching 63.6%, 28.1% and 35.6 % for CL, NL, and PSL, respectively within 24 h. These data revealed that

363 the liposomes exhibited significantly constant release profiles and AFT was successfully
364 loaded into the liposomes. However, the cumulative release of AFT in PSL at pH 5.5
365 reached to 101 % in 4 h, presenting a burst release phenomenon. The release profiles of
366 AFT from different liposomes apparently biphasic release processes, where rapid release
367 of the surface-adsorbed AFT was observed during the initial phase (first 4 h), followed by
368 a slow release profile for up to 24 h. The AFT release was increased significantly with the
369 pH decreased from 7.4 to 5.5 in case of PSL, and showed reasonably good pH-
370 responsiveness. But, in a physiological environment (pH 7.4), the encapsulated AFT was
371 released at a constant rate. It indicated that the AFT was well protected inside the liposome
372 bilayers at physiological pH. But in acidic condition (pH 5.5) cancer environment, the AFT
373 release was hastened. Therefore, the release of the PSL containing AFT was controlled by
374 the environmental pH. This phenomenon are consistent with the obtained results of
375 doxorubicin release at various pH values [27]. The constant release rate of AFT may
376 conserve a constant contact of the drug to the cancer cell resulted in improved antitumor
377 activity and helpful for drug delivery applications. The PSL system has the greatest
378 potential to improve cancer therapy efficacy. To fit the release kinetics of AFT from
379 liposomes at pH 5.5 and 7.4, different kinetic models viz. Peppas, Higuchi, zero order and
380 first order were exploited to predict the drug release profile. These models depend on the
381 diffusion equations, which based on the composition of liposomes and release conditions.
382 It was reported that the release of the drug from liposomes could be allocated in three
383 different mechanisms: diffusion, erosion and diffusion-erosion [28]. It was found that the
384 results were supported by the Korsmeyer-Peppas model at pH 7.4, which it presented the
385 highest value of R^2. Moreover, the values of n are 0.460, 0.681, 0.431 and 0.599 for CL,

386 NL, PSL and PSL (pH 5.5), respectively, indicated a non-Fickian diffusion kinetics ($0.5 <$
387 $n < 1$) [28]. PSL ($n=0.431$) exposed Fickian diffusion due to slow release at neutral
388 condition [28]. Subsequently, it is concluded that the drug release mechanism was mainly
389 owing to the combination of diffusion and erosion of the liposomes containing AFT (Table
390 4).

391 Moreover, the release profiles of the three AFT-loaded liposomes could be divided
392 into two phases, the first phase from 1 to 4 h and the second phase from 6 and 24 h. The
393 fitting parameters derived from korsmeyer-Peppas were listed in Table 5. n is the release
394 exponent indicating the drug release mechanism and k reflected the rate constant of the
395 release. At pH 7.4, n values of liposomes in the first phase were higher than 0.43, indicating
396 the release behavior of AFT followed a combination of diffusion and erosion control. In
397 the second stage, n values of liposomes were below 0.43, except NL, representing a
398 combination of diffusion and erosion mechanism. The k values for PSL at pH5.5 were
399 much higher than those of pH 7.4, demonstrating the highest release rate in an acidic
400 environment. The difference between k values of the first and second stage were nearly the
401 same, which indicated that the AFT release rate was comparatively slow in a neutral
402 environment.

403

404 3.8. Cell proliferation assay, WST-1

405 In general, it is essential to screen and confirm that the antitumor drugs are potent
406 and efficient for cancer therapy. Therefore, the potency of AFT was evaluated in
407 comparison with selected drugs depending on their activities against lung cancer in an *in*
408 *vitro* cell-based assay. Half-maximal inhibitory concentration (IC_{50}) of these drugs was

attained from an experimentally derived dose-response curve. In this study the cytotoxicity was evaluated with a WST-1 assay in H-1975 cells. The cells were incubated with AFT, paclitaxel, carboplatin and gemcitabine for 24 h. As shown in Fig. 7, the results detected that effect of AFT and paclitaxel on H-1975 cells had dose-dependent manner. On the contrary, the data displayed minor cytotoxicity against H-1975 cells, even up to the highest doses of carboplatin and gemcitabine. The IC_{50} values for AFT and paclitaxel were 20 and 25 µM, respectively. Particularly, by increasing the concentrations of AFT to 40 µM, H-1975 cells exhibited higher sensitivity than paclitaxel. The cell viability dropped to 2% with 40 µM of AFT and 50% with paclitaxel. Further increasing the concentration of AFT up to 80 µM, the insignificant reduction in the cell viability was observed (Fig. 7). Thus, *in vitro* anticancer activity revealed that AFT had potent cytotoxic (IC50 value; 20 µM) as compared to other drugs.

The cell toxicity of the best liposomes PSL, NL, and CL was also measured by a WST-1 assay on H-1975 cells (data not shown). Unfortunately, the reduction of cell viability (H-1975 cells) at any AFT concentrations did not recorded. This behavior confirmed that the WST-1 assay failed to detect any reduction in viable cell numbers. In contrast, the cytotoxicity (dose-dependent) was detected by microscopic examination using 1-80 µM of PSL, NL, and CL. Accordingly, the intracellular vacuoles and cell aggregates at concentrations from 1 to 5 µM was appeared. Further increasing the concentrations from 10 to 80 µM, indefinite aggregates of damaged and dying cells were perceived. The order of liposomes to kill H-1975 cell was followed as PSL > NL > CL. Therefore, AFT-loaded PSL at concentrations less than 10 µM were performed in the next study.

3.9. Annexin-V apoptosis assay

Apoptosis-inducing influence of AFT loaded-PSL formulation was evidenced by Annexin V/PI protocol. The extent and the nature of the induced cell death were analyzed by flow cytometry. H-1975 cells were incubated with various concentrations of AFT loaded-PSL (0.5 - 8 μM) for 24 h, which were selected based on WST-1 assay results. The amounts of the early apoptotic and the late apoptotic cells, with necrotic cells were determined after deduction of the proportion of spontaneous apoptosis. The results clearly revealed that the AFT loaded-PSL triggered both apoptosis in H-1975 cells (Fig. 8A).

The quantities of apoptotic cells increased from 55 to 58.9 % after exposure to 0.5 to 1 μM of AFT loaded PSL. However, increasing the concentration to 8 μM resulted in a reduction of the quantities of apoptotic cells from 30% at 3 μM to 9 % at 8 μM. Furthermore, high cell viability of 87.5 % of free liposomes was observed. Concerning the concentrations of AFT loaded-PSL at 3 to 8 μM, the proportions of necrotic cells increased as the number of apoptotic cells decreased. The proportions of necrotic cells increased from 3 to 90%, depending on the concentrations of AFT loaded-PSL at 0.5 and 8 μM (a dose-dependent manner) (Fig. 8B). Consequently, AFT at a concentration of 2.0 μM was selected due to high apoptotic activity for further cytotoxicity studies using different lung cancer cell lines.

Moreover, the cell viability of AFT loaded-PSL after H-1975 cells were incubated for 48 and 72 h in addition to 24 h also was investigated (Fig. 9). The significant cytotoxic effect in H-1975 cell at a concentration of 2 μM of AFT loaded-PSL, with the total cell death proportion exceeding 78, 80 and 84 % after 24, 48 and 72 h, respectively. The cytotoxic effect of the AFT-PSL formulation at a concentration of 2 μM was mainly due to induced apoptosis, with slight necrosis. For comparison, the cell viability of free

liposomes at 72 h was 90 %. These results revealed that no significant difference in the cell death after 24 and 48 h of exposure with H-1975 cells ($p > 0.05$). Therefore, 24 h of exposure was selected for further study. Free liposomes showed insignificance cytotoxic (apoptosis) after 24 and 48 h of exposure with considerable toxicity (necrosis) after 72 h of exposure.

Overall, the obtained results clearly revealed the greater anticancer activity of PSL as shown by a WST-1 assay and apoptosis assay. Therefore, 24 h of exposure was selected for further cytotoxicity study of AFT-loaded PSL, CL and NL by using different lung cancer cell lines. Hence, the anticancer activity of these liposomes was performed using Flow cytometric analysis in the three cell lines as H-1975, H-1650, and HCC-827 (Fig.10 A, B & C). This study was conducted to detect the level of apoptosis induced after incubation with various concentrations of 0.25, 0.5, 0.75, 1, and 2 µM of each liposomes for 24 h. While, dimethyl sulfoxide and free liposomes were used as the controls. The incubation of the cells with free liposomes did not induce notable cytotoxicity (data not shown). The viability of H-1975 cells decreased more significantly compared to H-1650 and HCC-827 cells ($p<0.05$). PSL produced highest cytotoxic effect in the different lung cancer cell lines (H-1975 cells and HCC-827) compared to NL and CL, when using concentrations 2 µM AFT (Fig. 10). Overall, the results clearly revealed the superior anticancer activity of PSL as shown by MTT assay and apoptosis assay.

Discussion

It has been reported that the cancer cells exhibited leaky vasculature with gap of ~100 nm, this allows the drug to leak out of the blood vessels and into the cancer cells [29]. Additionally, cancer cells have an impaired lymphatic system; therefore, substances such

as drugs loaded-liposome can be retained for a relatively longer time [30]. This behavior is commonly referred to EPR effect, which increases the exposure of tumor cells to drug action. The liposomes have been reported as a potential carrier to target cancer cells. The liposomes less 100 nm are able to escape the tumor vasculature and accumulate in the cells by passive targeting [31]. Moreover, the targeted liposomes were designed depending on the type of phospholipids used. In this study, it has been illustrated that modified liposomes as PSL can work as an effective carrier for delivery of AFT *in vitro*. Moreover, this carrier system presented significant antitumor activity. The desired liposomes can obtained by investigating different quantities of the drug to lipid ratios to detect the greatest encapsulated liposomes. Furthermore, the best liposomes in terms of vesicle size, PDI, ζ and EE were selected. The *in vitro* release study and cytotoxicity of the selected liposomes loaded AFT were examined. In addition, AFT is a potent antitumor drug used in clinical oncology against a lung tumor. However, AFT had low specificity, systemic toxicity and indiscriminating of the tumor and healthy tissues [14]. So AFT loaded-lipoosmes were developed for successful cancer therapy that decreases dose-limiting toxicity. In this study, a novel pH-sensitive liposomes-based AFT as targeted delivery (PSL) were used to target tumor cells. It has been observed that PSL has intensely improved the cytotoxicity in comparison to conventional liposomes (NL) or cationic liposomes (CL). Kraft *et al* observed that CL or PSL could accumulate in the lung cells more, compared with NL [32]. PSL exposed to the destabilization behavior under acidic condition, which lead to rapid release of its content. It is interesting that the tumor tissues are relatively acidic compared to the normal tissue site [19-21]. The main difference between these two liposomes is the composition of phospholipid used. In general, three lipid components: DSPC, DOPC, and

DOPE. DSPC were used. The rationale for the selection of DSPC was its stability against chemical degradation due to saturated lipid, which reduces the drug leakage from liposomes on storage and in vivo transit. To increase the fluidity of liposomal membrane, DOPC was selected due to its high fluidity at room temperature (transition temperature (T_m)= −20°C). While, T_m of DSPC is +55 °C, which remains in the gel phase [33]. Moreover, DOPE was combined to provide fusogenic characters to the liposomes, due to the formation of an inverted hexagonal phase upon destabilization of membranes at a mildly acidic pH [34]. Theses lipids possess various chain lengths and degrees of saturation, which can produce fine-tune the membrane dynamics and phase properties [35]. The main composition of CL is DOTAP, which is considered as a cationic phospholipid. While PSL composed from pH-sensitive phosphlipid (CHEMS). The film hydration method has been used to actively entrap AFT into liposomes with relatively high efficiencies and small vesicle size (<100 nm) [36]. The PDI values of the obtained liposomes are less than 0.3 indicating narrow size distribution. The higher ζ, of the obtained liposomes provoked the potential stability of a liposome. Patil *et al* investigated the influence of ζ on the cellular uptake of cerium oxide nanoparticles in A549 lung adenocarcinoma [37]. Thus, the charged surface of liposomes has ability to attach the cell membrane. Furthermore, to obtain the liposomes with the highest EE%, the best ratio of drug to phospholipid was selected for further studies. Accordingly, the highest EE% of AFT reached to 43.20%, 50.20%, and 52.01% for NL, PSL, CL, respectively at the 1:0.5 ratio of lipid to the drug. Nallamothu *et al* 2006 indicated that the high EE% of combretastatin A4 was obtained by increasing the drug to lipid ratios. By using 1:10 to 2:10 of combretastatin A4 to lipid ratios, the amount of the drug increased from 1.05 mg/ml

to 1.55 mg/ml, respectively. When the drug to lipid ratios was further increased to 4:10, the EE% of the drug did not increase [38]. Thus, the best liposomes were subjected to stability study, they exhibited better stability at 4°C or at 25°C after storage for 1 month. CL showed the highest stability in term of EE%, particle size and zeta potential. This effect is due to the inclusion of DOTAP in the liposomes, which decreases the rigidity of the liposomes with good loading capacity. *In vitro* drug release data revealed that PSL and NL exposed sustained release profiles due to the presence of DSPC (T_m), which lead to a decrease in leakage of AFT in the circulation or extracellular environment. But in case of CL, AFT exhibited high release rate compared with the other liposomes, at pH 7.4. This is due to the complete protontion of DOTAP at pH 7.4 [39]. By contrast, the fast drug release profile of AFT was found after addition PSL in acidic media, which reached to 100% after 4 h. The PSL undergoes destabilization at pH 5.5 and acquire fusogenic properties, thus tended to rupture and quickly release of AFT. The fusogenic performance of PSL is due to the presence of DOPE in the lipid layer, which forms a hexagonal structure instead of a bilayer structure after dispersion in aqueous media. Düzgünes *et al* showed that liposomes composed of CHEMS had high stabilize of EE calcein at pH 7.4 and undergo destabilization and irreversible aggregation under acidic pH [40]. According to the kinetic models, the release of AFT at pH 7.4 displayed release with Korsmeyer-Peppas model. This effect is due to early rapid release followed by slow release of the liposomes [41]. In case of the release pattern of PSL at pH 5.5, AFT release was quite faster with Korsmeyer-Peppas model. This behaviour because AFT exists liposomal membrane, which leaks out at a faster rate in acidic condition [42].

Therefore, it was confirmed that the pH-sensitive point in the liposome is close to 5 (the tumor microenvironment). PSL might release their content in the acidic environment of the tumor tissues quickly. Therefore, the PSL were fabricated in the current study to achieve a certain active targeting toward the tumor. The TEM of PSL revealed uniform, homogenous and spherical-shaped liposomes with a smooth surface.

The potency of free AFT was compared with selected drugs depending on their activity against lung cancer. The cell toxicity was evaluated by WST-1 using H-1975 cells. The WST-1 assay showed that AFT is more effective as a cytotoxic agent compared to other compounds used in lung cancer treatments (H-1975 cells). Furthermore, the anti-proliferative effect of AFT on H-1975 cells was investigated at various concentrations for 24 h. The results indicated that the inhibition of cell viability AFT had concentration-dependent manners. Moreover, anticancer activity of the obtained liposomes was also investigated using and H-1975 cells. Unfortunately, WSR-1 assay failed to detect the anticancer activity of the obtained liposomes due level of interference. However, a detailed characterization of this interference was not undertaken here. Therefore, the levels of cell viability between each liposomes were measured by using flow cytometry analysis after Annexin V/PI staining. The results of flow cytometry after the treatment of cells with the AFT loaded-PSL using different concentrations exhibited a comparable level of cell intensity. It was clearly indicated that the uptake of AFT loaded-PSL by H-1975 cells was higher than free AFT. The results revealed a marked decline in cell viability with AFT loaded-PSL up to 60.4% of cell apoptosis at 1 µM after 24 h. The free AFT resulted in apoptosis in 11.88% of the cells after 24 h. The low cytotoxic effect of free AFT could be attributed to the low cellular uptake and poor trans-membrane permeability. Of the three

cancer cell lines tested, H-1975 cells appeared more sensitive to the liposomes. Particularly, the cytotoxicity of PSL is high compared with that of CL and NL. It is possible that PSL released AFT in response to the lowered pH in the endosome, and thus facilitated diffusion of the released AFT from the endosome to the cytosol. It has been suggested that pH-sensitive liposomes are internalized more efficiently than non-pH-sensitive formulations [43]. It is notable that the destabilization of PSL at the endosomal demonstrated that the efficacy of PSL depends on the pH of the tumor tissues [34]. Additionally, the liposomes containing CHEMS release their contents into the cytoplasm from 5 to 15 min upon their incubation with the cells [44]. The destabilization of PSL induced by acidification of the endosomal lumen represents the most important stage in the process of intracellular delivery. Carvalho *et al* developed cisplatin loaded-PSL to treat the SCLC. Compared with free cisplatin, the cytotoxicity of this PSL was significantly enhanced [7]. Kim *et al* developed a PSL with an efficient and targeted delivery system for gemcitabine, and represent a useful, novel treatment approach for tumors that overexpress EGFR [45]. More, the cationic liposomes containing paclitaxel composed of DOTAP were able to significantly decrease tumor perfusion and vascular diameter and the progress of A-Mel-3 melanoma in mouse models [46]. The association of cationic liposomes with surface membrane is due to the presence of anionic glycoproteins, such as sialic acid rich glycoproteins [47]. Furthermore, pH-sensitive liposomes containing cytarabine have been shown greatly antitumor effectiveness in both human HepG2 hepatoma cells and normal human liver L02 cells compared to non-pH-sensitive liposomes [48]. These promising results are required further *in vivo* analysis to understand the biodistribution profile of AFT loaded PSL to achieve new targeted-formulation for the tumor therapy.

4. Conclusion

In this work, a novel AFT-loaded PSL for targeted therapy of lung cancer (NSCLC) were developed. For comparison purpose, AFT-loaded NL, CL and PSL were successfully designed. The obtained liposomes showed small particle less than 100 nm with a low PDI (<0.27) and acceptable zeta potential with a spherical shape. The highest EE% values of the liposomes were achieved according the following order: CL>PSL>NL. The selected liposomes were stable at 4 and 25°C for 1 month. The PSL, CL and NL showed slow release profiles in pH 7.4. However, in acidic pH values, PSL exhibited fast release, which improved its tumor targetability. The selected liposomes revealed efficiency on cancer cells (NSCLC). Moreover, AFT-loaded PSL inhibited the cell growth of lung cancer cells more efficiently than free AFT, CL and NL based on using Annexin V assay. The obtained data indicate that AFT-loaded PSL is a promising a targeted drug delivery for cancer therapy.

Acknowledgements

The authors extend gratitude to the Research Centre of King Faisal Specialist Hospital for the fruitful collaboration, and convey special thanks to and gratefully acknowledge the help and expertise of Ms. Zakia Shanawani. This research project was supported by a grant from ‘‘the Research Center of the Female Scientific and Medical Colleges’’, Deanship of Scientific Research, King Saud University.

References

1. Y. Bahader, and A.-R. Jazieh, Epidemiology of lung cancer, Ann. Thorac. Med. 3 (2008) 65-67.
2. O. Alamoudi, Prevalence of respiratory diseases in hospitalized patients in Saudi Arabia: A 5 years study 1996-2000, Ann. Thora. Med. 1 (2006) 76-80.
3. C.R. UK, Lung cancer and smoking. UK. Cancer Stats. Cancer Research UK. 2008. Sep., available form: http:// www.info.cancerresearchuk.org/cancerstats/ Lung/html.

4. K.A. Al-Turki, N.A. Al-Baghli, A.J. Al-Ghamdi, A.G. El-Zubaier, R. Al-Ghamdi, Prevalence of current smoking in Eastern province, Saudi Arabia, East Mediterr. Health J. 16 (2010) 671-667.
5. M.R. Davidson, A.F. Gazdar, B.E. Clarke, The pivotal role of pathology in the management of lung cancer. J.Thorac. disease, 5 (2013) S463-S478.
6. A.Goel, S. Baboota, J.K. Sahni, J. Ali, Exploring targeted pulmonary delivery for treatment of lung cancer. Int. J. Pharm. Invest. 3 (2013) 8-14.
7. T.C. Carvalho, S.R. Carvalho, J.T. McConville, Formulations for pulmonary administration of anticancer agents to treat lung malignancies, J. Aerosol Med. Pulm. Drug Deliv. 24 (2011) 61-80.
8. G. Pilcer, and K. Amighi, Formulation strategy and use of excipients in pulmonary drug delivery, Int. J. Pharm. 392 (2010) 1-19.
9. S. Anabousi, U. Bakowsky, M. Schneider, H. Huwer, M. Lehr, C. Ehrhardt, In vitro assessment of transferrin-conjugated liposomes as drug delivery systems for inhalation therapy of lung cancer, Eur. J. Pharm. Sci. 29 (2006) 367-374.
10. T. Mukohara, Mechanisms of resistance to anti-hu C man epidermal growth factor receptor 2 agents in breast cancer, Cancer Science, 102 (2011) 1-8.
11. G.Metro, and L. Crinò, The LUX-Lung clinical trial program of afatinib for non-small-cell lung cancer, Expert rev. anticancer ther. 11 (2011) 673-682.
12. F. Solca, G. Dahl, Z. Aoephel, G Bader, M. Sanderson, K. Clein, O. Kraemer, F. Himmelsbach, E. Haaksma, G.R. Adolf, Target binding properties and cellular activity of afatinib (BIBW 2992), an irreversible ErbB family blocker, J. Pharmacol. Exp. Ther. 343 (2012) 342-350.
13. V. Hirsh, Afatinib (BIBW 2992) development in non-small-cell lung cancer, Future Oncology 7 (2011) 817-825.
14. S.C. Coelho, G.M. Almeida, M.C. Pereira, F.S. Silva, Functionalized gold nanoparticles improve afatinib delivery into cancer cells, Expert Opin Drug Deliv, 13 (2016) 133-41.
15. Y. Malam, M. Loizidou, A.M. Seifalian, Liposomes and nanoparticles: nanosized vehicles for drug delivery in cancer, Trends Pharmacol sci. 30 (2009) 592-599.

16. S. Martins, B. Sarmento, D.C. Ferreira, E.B. Souto, Lipid-based colloidal carriers for peptide and protein delivery-liposomes versus lipid nanoparticles, Int. J. nanomedicine, 2 (2007) 595-607.
17. A.S. Ulrich, Biophysical aspects of using liposomes as delivery vehicles, Bioscience reports 22 (2002) 129-150.
18. T. Liu, H. Choi, R. Zhou, I.W. Chen, RES blockade: A strategy for boosting efficiency of nanoparticle drug, Nano Today, 10 (2015) 11-21.
19. Y. Duan, L. Wei, J. Petryk, T.D. Ruddy, Formulation, characterization and tissue distribution of a novel pH-sensitive long-circulating liposome-based theranostic suitable for molecular imaging and drug delivery, Int. J. Nanomedicine 11 (2016) 5697-5708.
20. M. Chang, S. Lu, F. Zhang, T. Zuo, Y. Guan, T. Wei, W. Shao, G. Lin, RGD-modified pH-sensitive liposomes for docetaxel tumor targeting, Colloids Surfaces B 129 (2015) 175-182.
21. Y. Zhang, Y. Wang, Y. Yang, S. Liu, Q. Ruan, X. Zhang, J. Tai, T. Chen, High tumor penetration of paclitaxel loaded pH sensitive cleavable liposomes by depletion of tumor collagen I in breast cancer, ACS Appl. Mater. Interfaces 7 (2015) 9691-9701.
22. S.S. Guan, J. Chang, C.C. Cheng, T.Y. Luo, C.C. Wang, S.H. Liu, Afatinib and its encapsulated polymeric micelles inhibits HER2-overexpressed colorectal tumor cell growth in vitro and in vivo, Oncotarget. 5 (2014) 4868-4880.
23. Y. Fan, C. Chen, Y. Huang, F. Zhang, G. Lin, Study of the pH-sensitive mechanism of tumor-targeting liposomes, Colloids Surf. B Biointerfaces, 151 (2017) 19-25.
24. S. Dash, P.N. Murthy, L. Nath, P. howdhury, Kinetic modeling on drug release from controlled drug delivery systems, Acta Pol. Pharm. 67 (2010) 217-23.
25. R. Vejendla, C. Subramanyam, G. Veerabhadram, New RP-HPLC method for the determination of afatinib dimaleate in bulk and pharmaceutical dosage forms, Indo-American J. Pharmaceut. Res. 5 (2015) 2015-2111.
26. F. Meng, R. Cheng, C. Deng, Z. Zhong, Intracellular drug release nanosystems, Materials Today, 15 (2012) 436-442.

27. Y. Zhao, W. Ren, T. Zhong, S. Zhang, Tumor-specific pH-responsive peptide-modified pH-sensitive liposomes containing doxorubicin for enhancing glioma targeting and anti-tumor activity, J. Controlled Rel. 222 (2016) 56-66.
28. N.A. Peppas, J.J. Sahlin, A simple equation for the description of solute release. III. Coupling of diffusion and relaxation, Int. J. Pharm.57 (1989)169-172.
29. H.M. Mansour, C.-W. Park, D. Hayes, Nanoparticle lung delivery and inhalation aerosols for targeted pulmonary nanomedicine. 2013: CRC Press, Taylor & Francis Group: Boca Raton, FL, USA.
30. H. Maeda, H. Nakamura, J. Fang, The EPR effect for macromolecular drug delivery to solid tumors: Improvement of tumor uptake, lowering of systemic toxicity, and distinct tumor imaging in vivo, Adv. drug deliv. Rev. 65 (2013) 71-79.
31. M. Brandl, Liposomes as drug carriers: a technological approach, Biotechnol Annual Rev. 7 (2001) 59-85.
32. J.C. Kraft, J.P. Freeling, W. Zang, R.J. Ho, Emerging research and clinical development trends of liposome and lipid nanoparticle drug delivery systems. J Pharm. .Sci. 103 (2014) 29-52.
33. A. Fahr, P. van Hoogevest, S. May, B.Nergstrand, S. Leigh, Transfer of lipophilic drugs between liposomal membranes and biological interfaces: consequences for drug delivery, Eur. J. Pharm. Sci. 26 (2005) 251-265.
34. R. Karanth, R.S. Murthy, pH-Sensitive liposomes-principle and application in H.cancer therapy, J. Pharm. Pharmacol. 59 (2007) 469-483.
35. U. Michaelis, H. Haas, Targeting of cationic liposomes to endothelial tissue, in Liposome Technology, G. Gregoriadis, Editor. 2006, Informa Healthcare, 151-170.
36. G.M. Jensen, T.H. Bunch, Conventional liposome performance and evaluation: lessons from the development of Vescan, Journal of liposome research, 17(2007) 121-137.
37. S.Patil, S. Aandberg, E. Heckert, W. Self, S. Seal, Protein adsorption and cellular uptake of cerium oxide nanoparticles as a function of zeta potential, Biomaterials, 38 (2007) 4600-4607.
38. R. Nallamothu, G.C. Wood, K.F. Kiani, L.A. Thoma, A targeted liposome delivery system for combretastatin A4: formulation optimization through drug loading and in vitro release studies, PDA J. Pharm. Sci. Technol, 60 (2006) 144.

707 39. N.J. Zuidam, Y. Barenholz, Electrostatic and structural properties of complexes
708 involving plasmid DNA and cationic lipids commonly used for gene delivery, Biochim
709 Biophys Acta, 1368 (1998) 115-128.
710 40. J.J. Sudimack, W. uo, R.J. Lee, A novel pH-sensitive liposome formulation containing
711 oleyl alcohol, Biochim Biophys Acta, 1564 (2002) 31-37.
712 41. C. Koutsoulas, N. Pippa, C. Demetzos, M. Zabka, Preparation of liposomal
713 nanoparticles incorporating terbinafine in vitro drug release studies J. Nanosci.
714 Nanotechnol. 14 (2014), 4529-4533.
715 42. S. Modi, B.D. Anderson, Determination of drug release kinetics from nanoparticles:
716 overcoming pitfalls of the dynamic dialysis method, Mol. Pharm. 10 (2013), 3076-
717 3086..
718 43. T. Ishida, Y. Okada, H. Kiwada, Development of pH-sensitive liposomes that
719 efficiently retain encapsulated doxorubicin (DXR) in blood, Int. J. Pharm. 309(2006)
720 94-100.
721 44. D.S. Collins, K. Findlay, C.V. Harding, Processing of exogenous liposome-
722 encapsulated antigens in vivo generates class I MHC-restricted T cell responses, J.
723 Immunol. 148 (1992) 3336-3341.
724 45. I.-Y Kim, Y.S. Kang, D.S. Lee, H.J. Park, E.K. Choi, Y.K. Oh, J.S. Kim, Antitumor
725 activity of EGFR targeted pH-sensitive immunoliposomes encapsulating gemcitabine
726 in A549 xenograft nude mice. J. Controlled Rel. 140 (2009) 55-60.
727 46. S. Strieth, M.E. Eichhorn, B. Sauer, B. Schulze, M. Teifel, U. Michaelis, M. Dellian,
728 Neovascular targeting chemotherapy: encapsulation of paclitaxel in cationic liposomes
729 impairs functional tumor microvasculature, Int. J. Cancer 110, (2004)117-124.
730 47. R. Weijer, M. Broekgaarden, M. Kos, R. van Vught, E.A. Rauws, E. Breukink, T.M.
731 van Gulik, G. Storm, M. Heger, Enhancing photodynamic therapy of refractory solid
732 cancers: combining second-generation photosensitizers with multi-targeted liposomal
733 delivery, J. Photochem. Photobiol. Chem. 23 (2015) 103-131.
734 48. L. Wang, D. Geng, H. Su, Safe and efficient pH sensitive tumor targeting modified
735 liposomes with minimal cytotoxicity, Colloids Surf B Biointerfaces 123 (2014) 395-
736 402.
737

Table 1

Compositions of different types of liposomes.

	Amount required (μmol/mL)		
Phospholipids*	NL	PSL	CL
DSPC	3	3	3
DOPC	10	7	7
DOPE	3	3	3
CHEMS	-	3	-
DOTAP	-	-	3

*NL: Non-targetin liposomes; CL: Cationic liposomes; PSL: pH-sensitive liposomes; DSPC: 1,2-distearoyl-sn-glycero-3-phosphocholine[18:0]; DOPC: 1,2-dioleoyl-sn-glycero-3-phosphocholine [18:1]; DOPE:1,2-dioleoyl-sn-glycero-3-phosphoethanolamine [18:1]; CHEMS: Cholesteryl hemisuccinate; DOTAP:1,2-dioleoy-3-trimethylammonium-propane Chloride salt (DOTAP)

Table 2

Precision of the developed method for analysis of AFT.

Nominal (µg/mL)	Concentrations Mean ± SD	CV%
0.01	0.01 ± 6.09	0.9266
0.05	0.05 ± 6.40	0.8051
0.1	0.1 ± 5.71	1.7143
0.25	0.25 ± 1.76	0.7076
0.5	0.5 ± 5.70	1.1404
1	1 ± 1.77	0.1763
2	2 ± 4.03	2.3016
5	5 ± 5.65	1.0731
10	10 ± 3.76	1.3577
20	20 ± 3.83	0.1992
25	25 ± 2.55	0.1102

SD: standard deviation; CV: Coefficient of variation percetage

Table 3

Repeatability for different levels of AFT (n = 3).

Concentration (µg/ml)	Mean ± SD[a]	Precision RSD[b] (%)	Accuracy (%)
Inter day			
0.1	99.98 ± 1.98	1.98	99.9
1	1000.72 ± 0.49	0.05	102
10	10000 ± 113.26	1.13	100.1
Intra-day			
0.1	100 ± 1.06	1.07	99.86
1	1000 ± 0.29	0.03	100.5
10	10000 ± 60.08	0.6008	100.2

a Standard deviation of the mean
b Relative standard deviation

Table 1

Release kinetics of AFT release from different liposomes.

pH media	Codes	Zero order	First order	Higuchi (Diffusion)	Korsmeyer Peppas	"n" value
pH 7.4	CL	0.691	0.559	0.871	0.940	0.460
	NL	0.928	0.731	0.988	0.994	0.681
	PSL	0.754	0.634	0.912	0.971	0.431
pH 5.5	PSL	0.647	0.486	0.835	0.889	0.599

Table 5

Drug release kinetics parameters derived from Korsmeyer Peppas.

pH media	Codes	$^{a}n_1$	$^{a}k_1$	$^{b}n_2$	$^{b}k_2$
	CL	0.675	16.987	0.168	37.619
pH 7.4	NL	0.681	3.606	0.527	5.434
	PSL	0.483	8.809	0.201	16.381
pH5.5	PSL	0.941	20.910	0.181	59.671

[a]The first stage is 0-4 h. [b]The second stage is 6-24 h.

827 **Fig. 1**

828

829

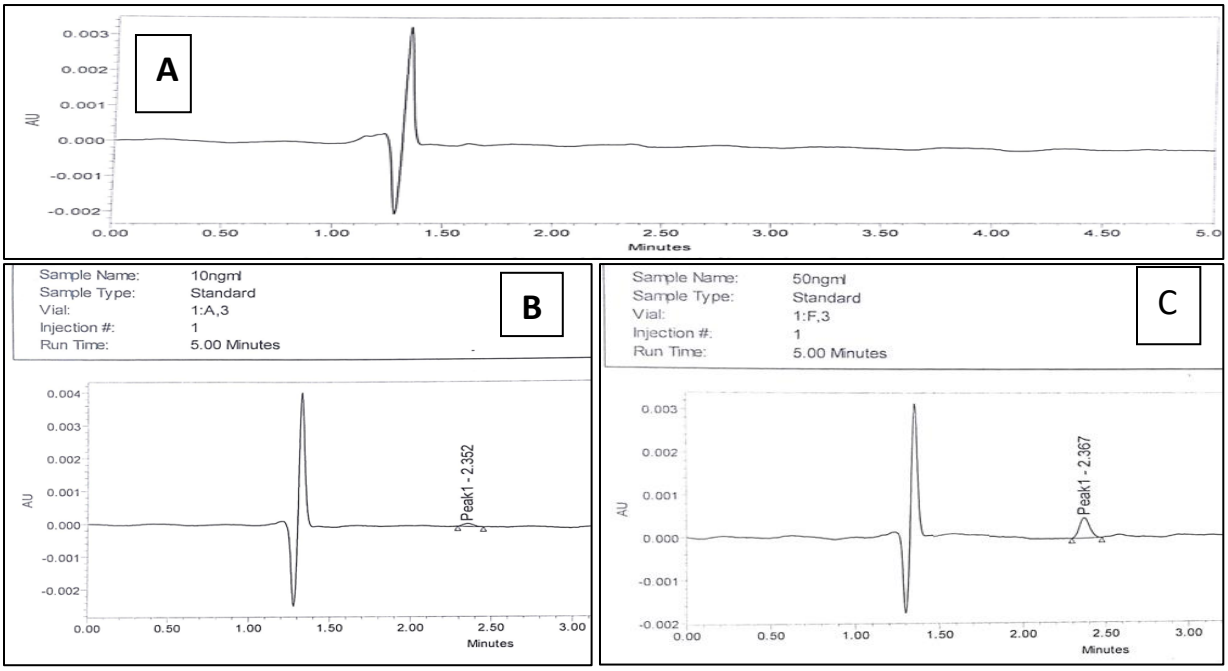

Fig. 1. HPLC chromatograms of the mobile phase (chromatogram A), and HPLC chromatograms of the mobile phase containing (B) 10 ng/ml and (C) 50 ng/ml afatinib.

830

831

832

833

834

835

836

837

838

839 **Fig. 2**

840

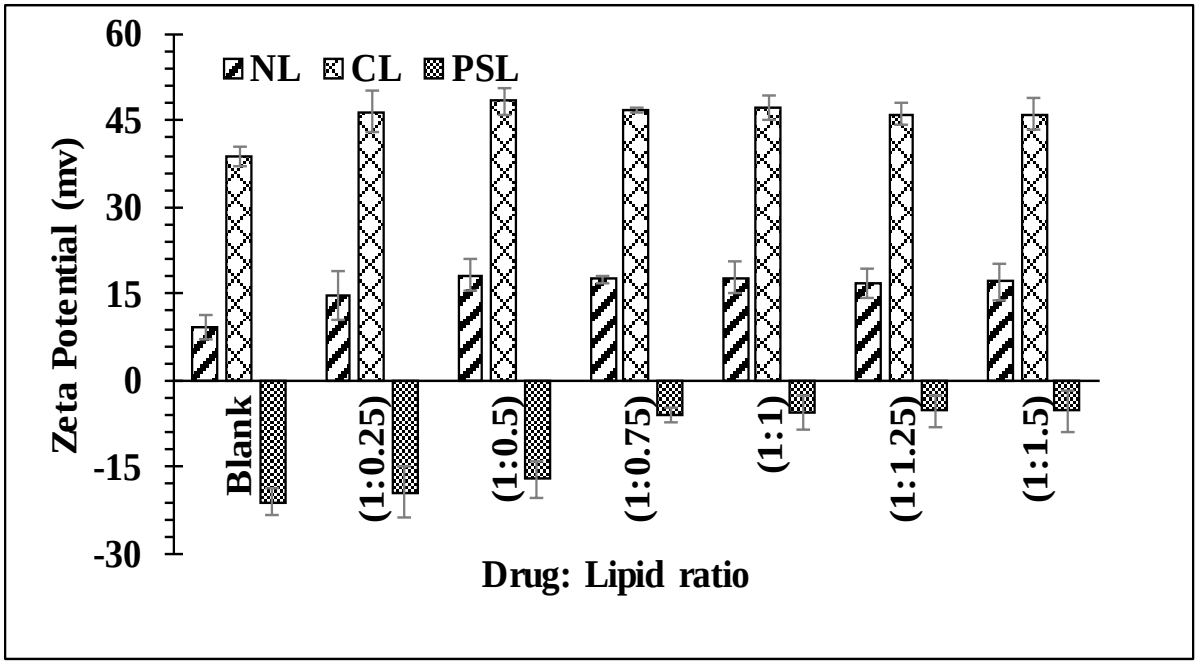

Fig. 2. Zeta potentials of afatinib-loaded liposomal formulations at different lipid to drug ratios.

841

842

843

844

845

846

847

848

849

850

851

852 **Fig. 3**

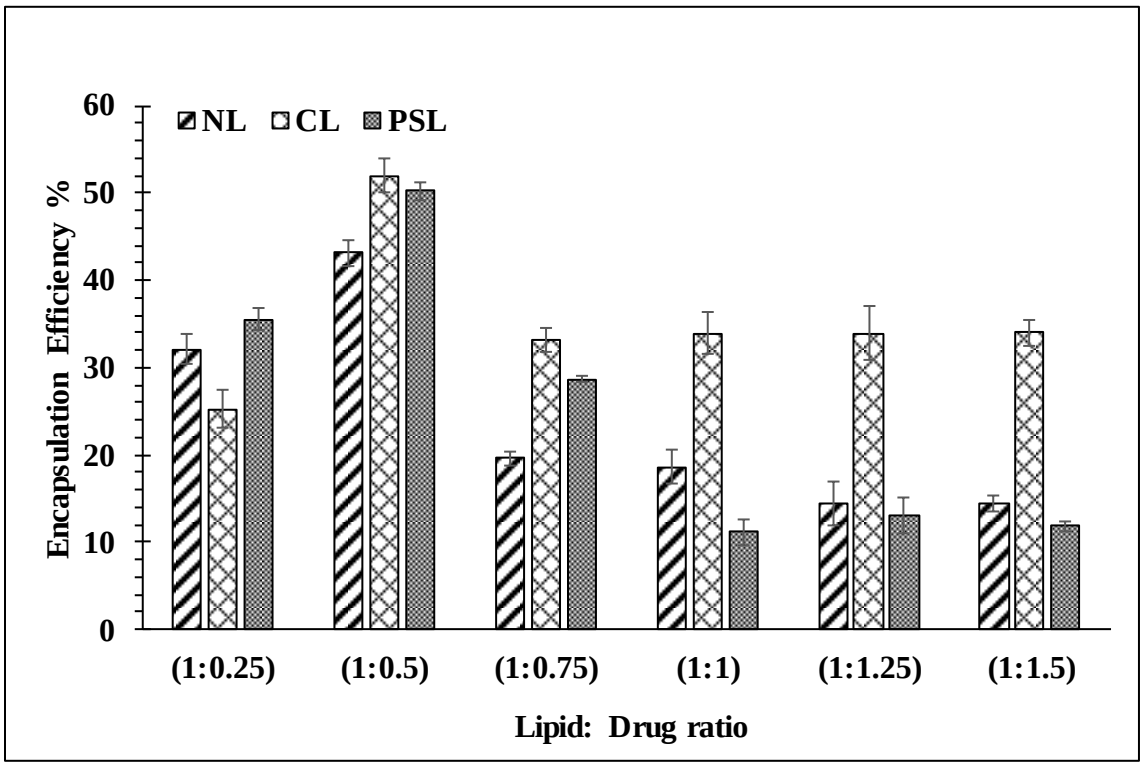

Fig. 3. EE% of afatinib-loaded different liposomal formulations with different lipid to drug ratios.

Fig. 4

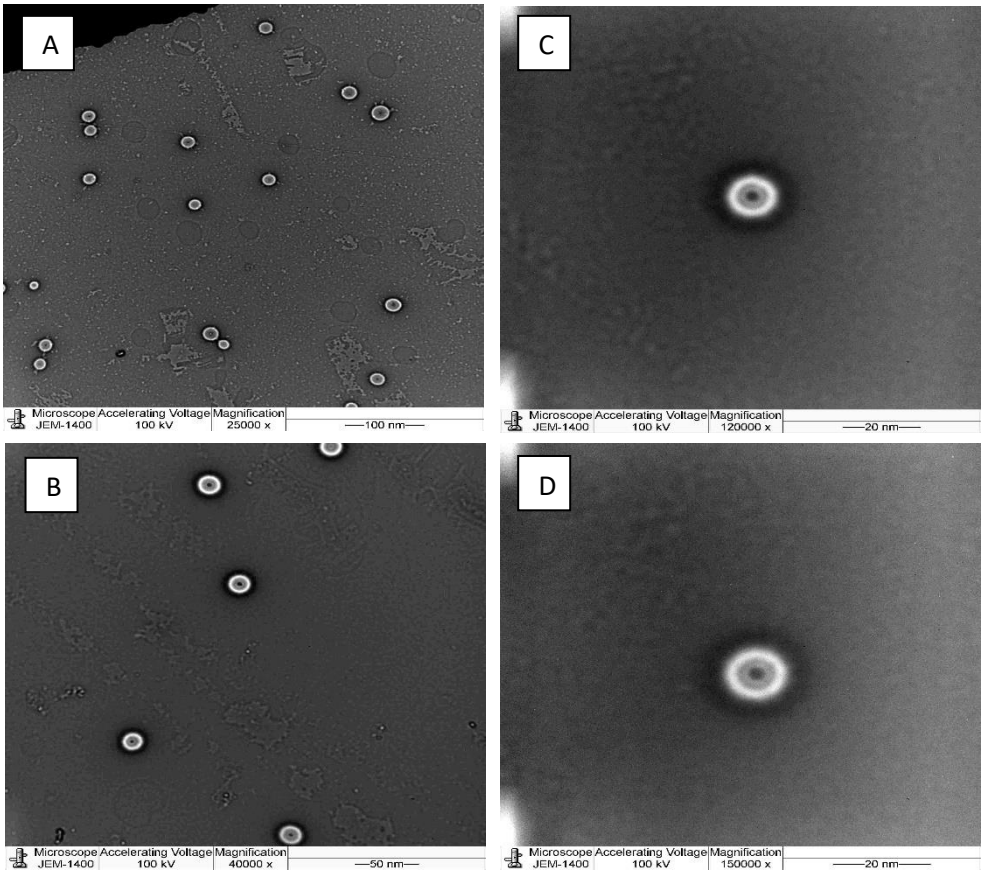

Fig. 4. TEM micrographs of the pH sensitive liposome at a drug to lipid ratio of 1:0.5 (PSL), using varied magnification power.

Fig. 5

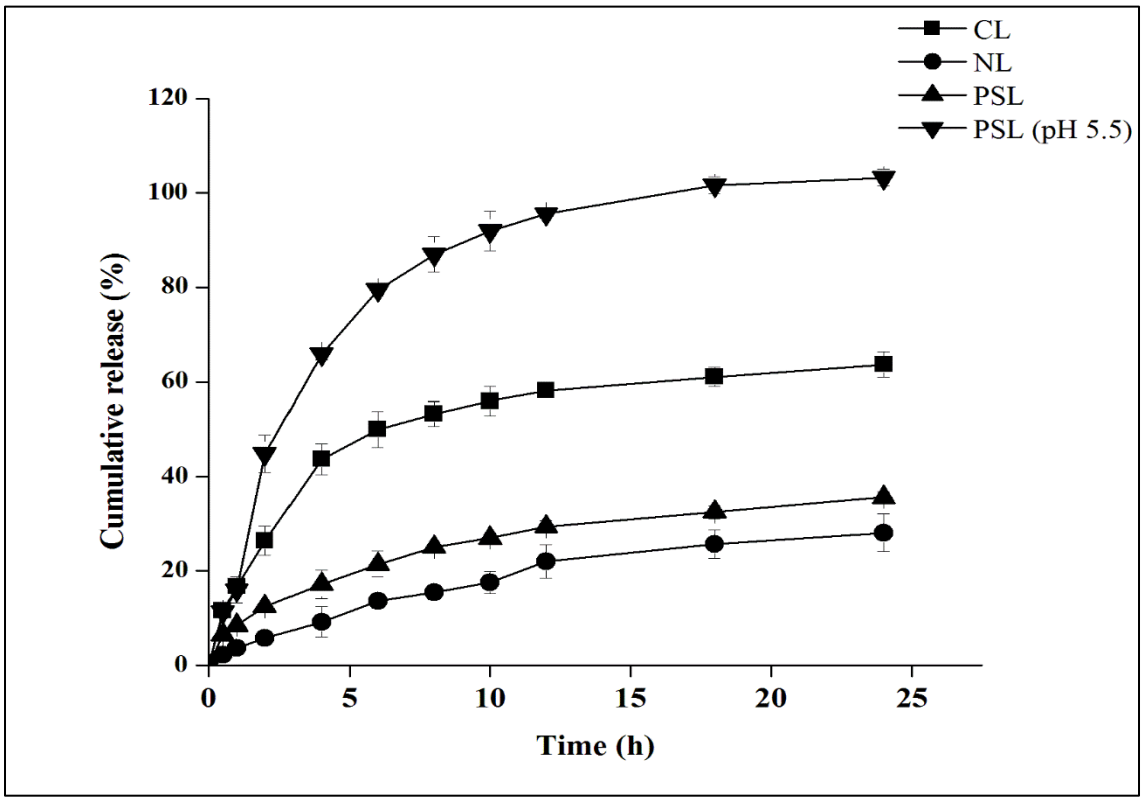

Fig. 5. *In vitro* release profiles of the liposomal formulations loaded with afatinib in phosphate-buffered saline containing 0.2% Tween 80 at pH 7.4 and pH 5.4. Values are presented as the mean ± SD.

Fig. 6

923

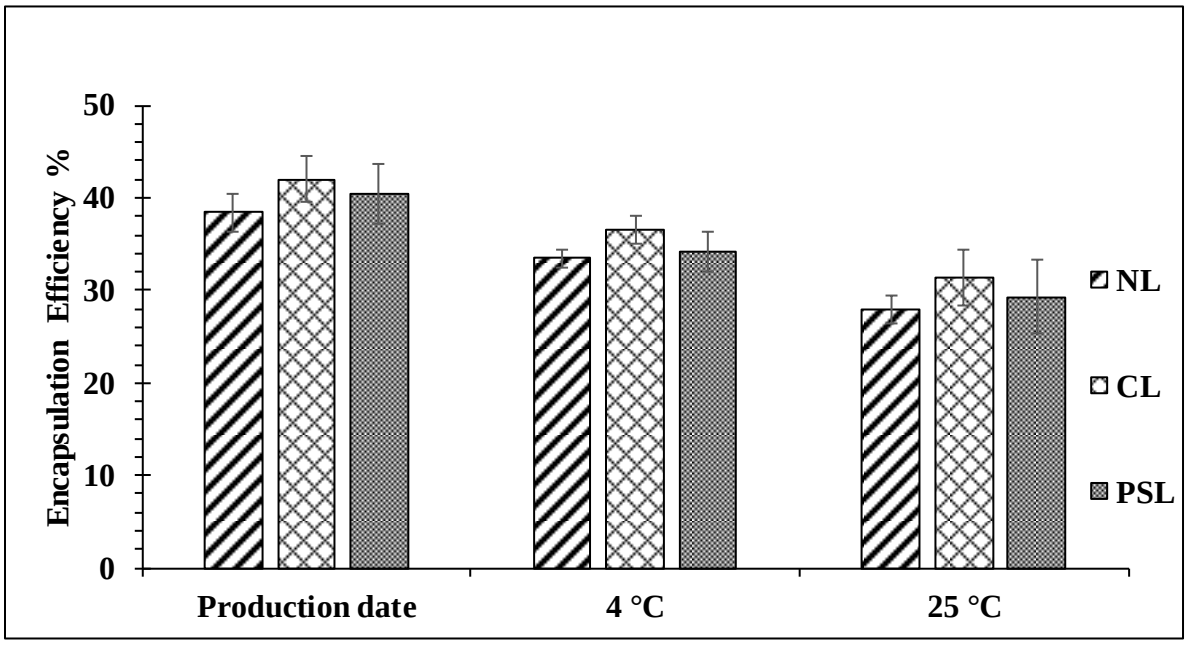

Fig. 6. EE % of afatinib at the ratio 1:0.5, following storage for one month at 4 and 25°C, of NL (nontargeting liposome), PSL (pH sensitive liposome) and CL (cationic liposome), P = 0.141.

924

925

926

927

928

929

930

931 **Fig. 7**

932

933

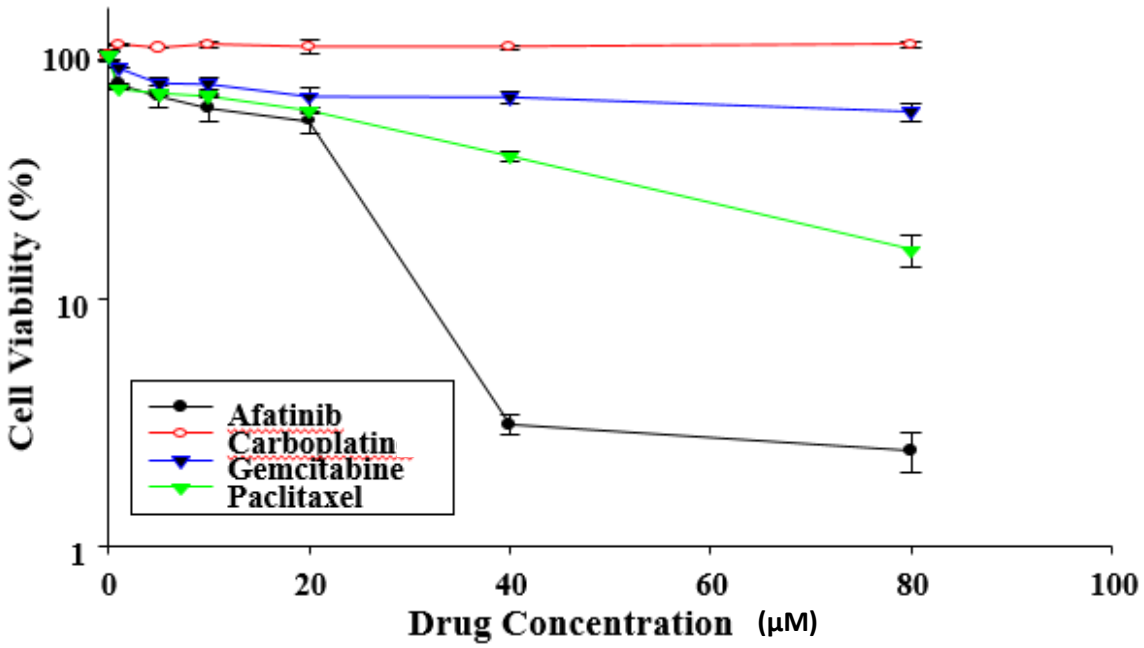

Fig. 7. Cytotoxicity of afatinib, carboplatin, gemcitabine and paclitaxel on H-1975 cells, as determined by a WST-1 assay. Cells were treated with varying concentrations of the drugs for 24 h. Results are from three independent experiments and are expressed as the mean ± SD.

Fig. 8

952

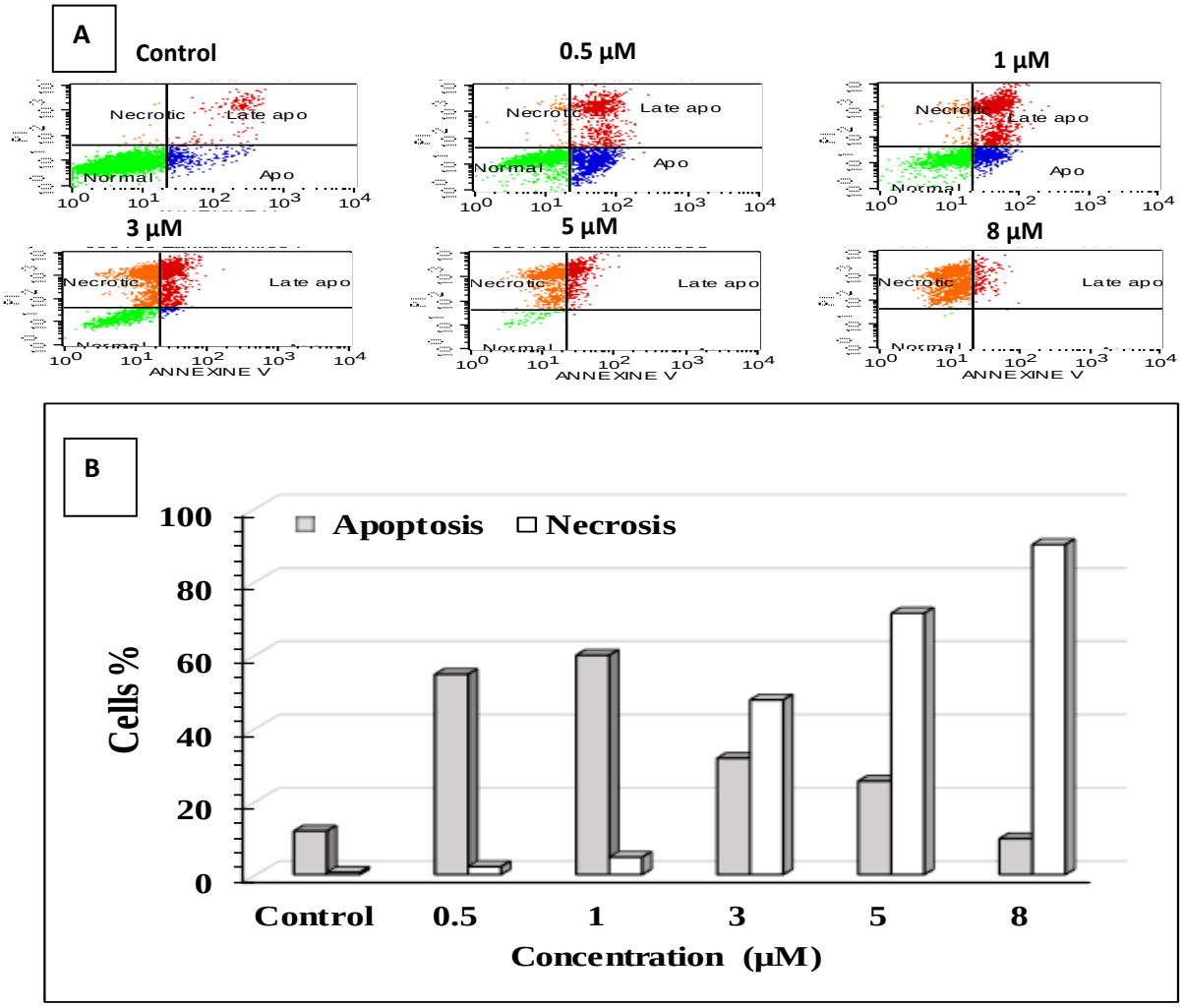

Fig. 8. H-1975 lung cancer cells were either treated with free liposomes, as controls, or challenged with Afatinib loaded liposomes (PSL2) for 24 hrs, and then the proportion of apoptosis and necrosis was analysed by Annexin V/PI-flowCytometry. four groups of cells, viable cells that excluded both Annexin V and PI (Annexin V/PI), bottom left; early apoptotic cells that were only stained with Annexin V (Annexin V+/PI), bottom right; late apoptotic cells that were stained with both Annexin V and PI (Annexin V+/ P+), top right and necrotic cells that were only stained with PI (Annexin V/PI+), top left. (A) Flow charts. (B) Histogram showing the percentage of induced apoptosis in H-1975cells.

953

954

955

Fig. 9

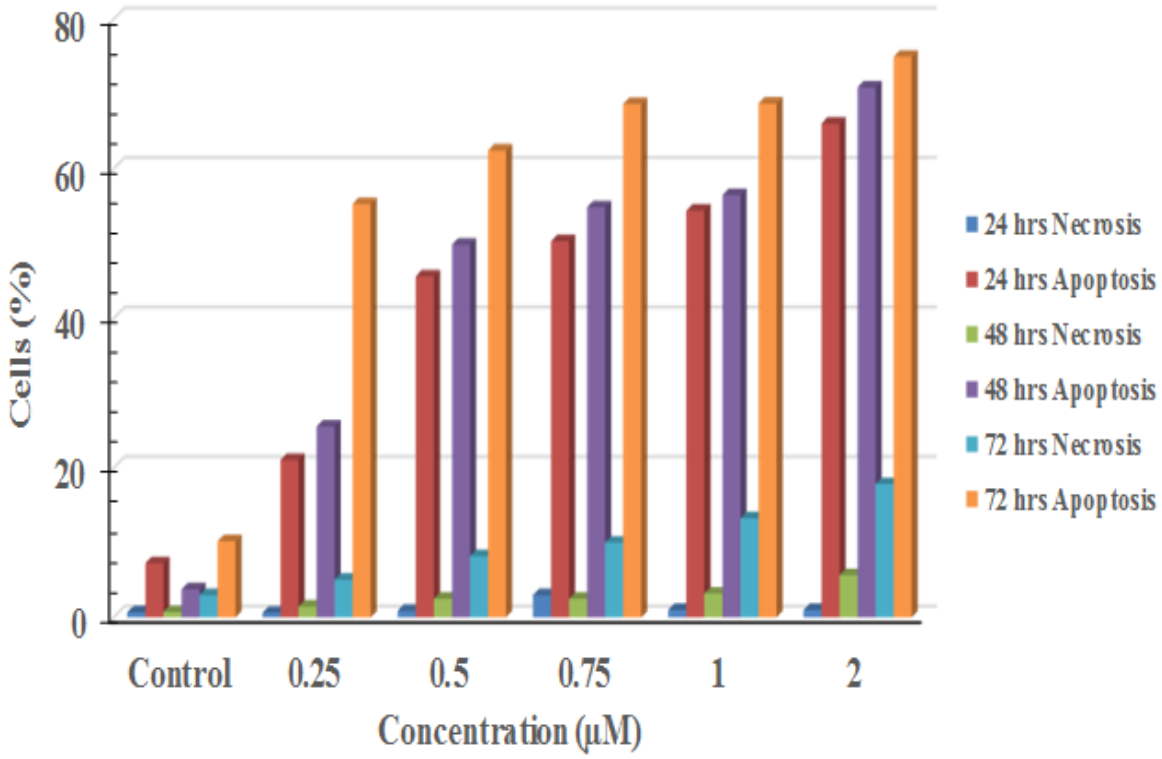

Fig. 9. H-1975 cells were challenged with pH-sensitive liposomes (PSL) (0.25-2 µM) for 24, 48 or 72 h, following which apoptosis was analysed with Annexin V/PI-flow cytometry. Each value represents the mean ± SD of three independent experiments performed in triplicate.

Fig. 10

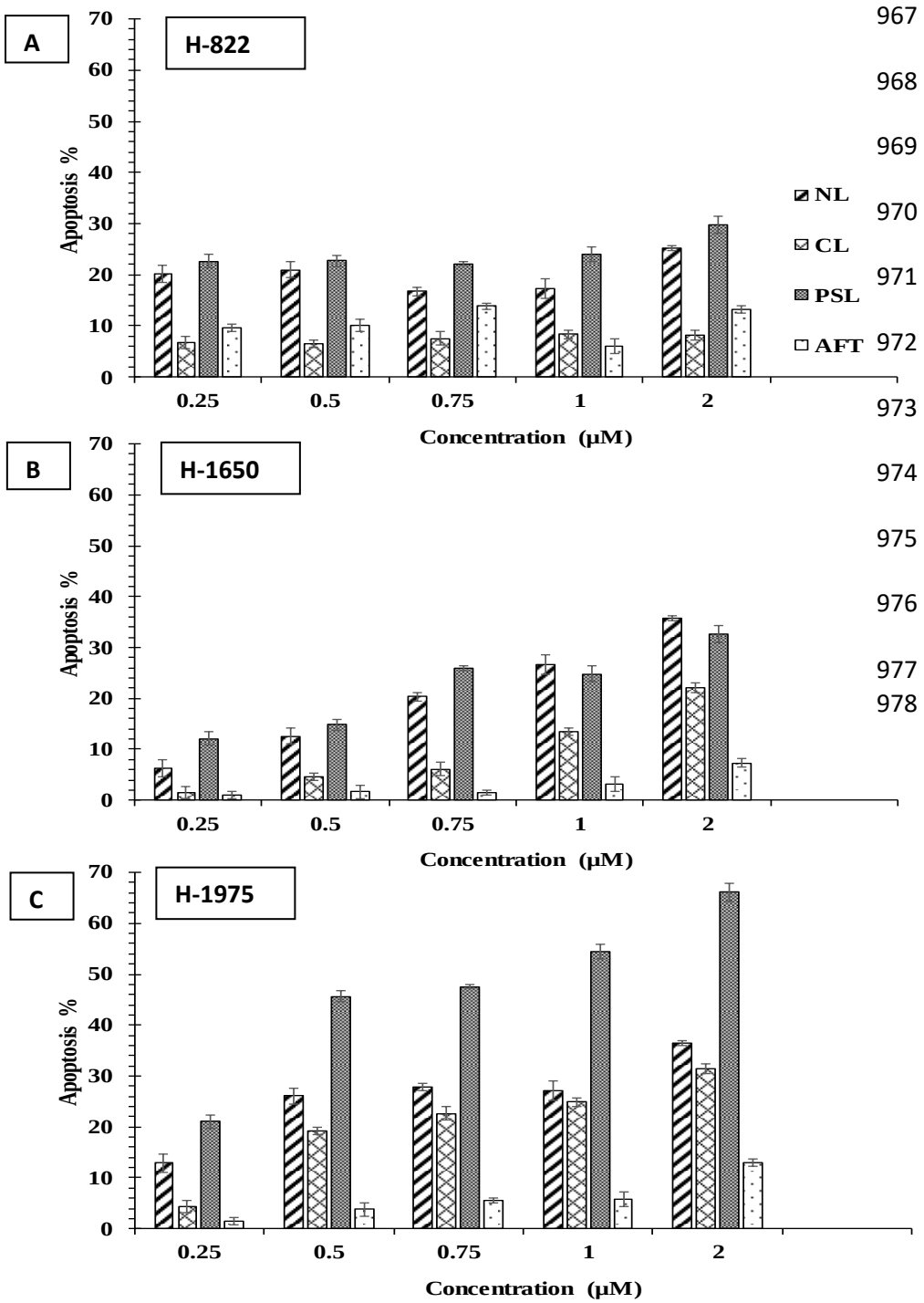

Fig.10. Non-small cell lung cancer cells were either treated with Blank Liposomes, as control, or challenged with AFT and AFT-loaded liposomes (PSL, NL, CL) for 24 h, following which the proportion of apoptotic cells was analysed using Annexin V/PI-flow cytometry. Histogram shows the percentage of induced apoptosis in H-1975 cells. Each point represents the mean ± SD of three independent experiments performed in duplicate.